applied sciences

MDPI

Article

Novel Predictive Model of the Debonding Strength for Masonry Members Retrofitted with FRP

Iman Mansouri [1], **Jong Wan Hu** [2,3,*] **and Ozgur Kisi** [4]

1 Department of Civil Engineering, Birjand University of Technology, Birjand 97175-569, Iran; mansouri@birjandut.ac.ir
2 Department of Civil and Environmental Engineering, Incheon National University, 12-1 Songdo-dong, Yeonsu-gu, Incheon 22012, South Korea
3 Incheon Disaster Prevention Research Center, Incheon National University, 12-1 Songdo-dong, Yeonsu-gu, Incheon 22012, South Korea
4 Center for Interdisciplinary Research, International Black Sea University, Tbilisi 0131, Georgia; okisi@ibsu.edu.ge
* Correspondence: jongp24@incheon.ac.kr; Tel.: +82-32-835-8463; Fax: +82-32-835-0775

Academic Editor: Patrick A. Fairclough
Received: 21 September 2016; Accepted: 1 November 2016; Published: 5 November 2016

Abstract: Strengthening of masonry members using externally bonded (EB) fiber-reinforced polymer (FRP) composites has become a famous structural strengthening method over the past decade due to the popular advantages of FRP composites, including their high strength-to-weight ratio and excellent corrosion resistance. In this study, gene expression programming (GEP), as a novel tool, has been used to predict the debonding strength of retrofitted masonry members. The predictions of the new debonding resistance model, as well as several other models, are evaluated by comparing their estimates with experimental results of a large test database. The results indicate that the new model has the best efficiency among the models examined and represents an improvement to other models. The root mean square errors (RMSE) of the best empirical Kashyap model in training and test data were, respectively, reduced by 51.7% and 41.3% using the GEP model in estimating debonding strength.

Keywords: debonding strength; FRP; masonry; gene expression programming; formulation

---

1. Introduction

Masonry buildings have been utilized from time immemorial and, these days, because of aging, material degradation, and structural variations, members' performances often need to be strengthened. In this case, fiber reinforced polymer (FRP) composites in the form of bonded laminates attached to the outside can be a lasting strengthening solution provided that they comply with the cultural value of the building [1]. The use of FRP material, however, causes novel and significant modeling problems [2,3], in spite of various material modeling plans that were extended in previous years achieving reproduction of the structural behavior of both un-strengthened and FRP-strengthened masonry structures [4,5].

A diversity of FRP strengthening systems has been indicated to develop the out-of-plane load-carrying capacity of masonry elements (e.g., [6–15]). Many experimental investigations have been performed with the purpose of studying the capability of using FRP in the strengthening of masonry structures (e.g., [4,16–18]). Similar experimental tests for monotonic or cyclic loading have been performed by Fam et al. [16], Al-Salloum and Almusallam [19], Wang et al. [20], and Stratford et al. [21]. Accardi et al. [22] proposed a local bilinear shear stress-slip law (bond behavior) between CFRP strips and calcarenite stone using an experimental study with three different bonded lengths (l_b):

50, 100, and 150 mm. Moreover, mathematical models have also been developed for improving the existing models to fit the experimental results better ([3,5,23]). Mansouri and Kisi [24] proposed the use of neural networks and neuro-fuzzy models for modeling the debonding strength of retrofitted masonry elements.

Failure modes observed in these investigations contain debonding of the FRP laminate from the masonry layer, tensile rupture of the FRP laminate, masonry crushing in the compression area, flexural-shear fracture near the support, sliding shear fracture along a bed joint, and localized masonry collapse. A very common fracture is created by bond loss of the FRP reinforcement, called as debonding failure. Debonding happens when the FRP is no longer adhered to the element because of a crack or separation of the fiber matrix and bond junction. This failure mode is often referred to as intermediate crack (IC) debonding [25]. The adhesive bonded joint analyzed, illustrated in Figure 1, can be noticed as a simple and generic model of FRP-strengthened structures to understand stress transfer and debonding behavior. There are various analytical models for calculating the debonding strength of members with FRP shear retrofit in the literature (e.g., models in Section 2 of this paper).

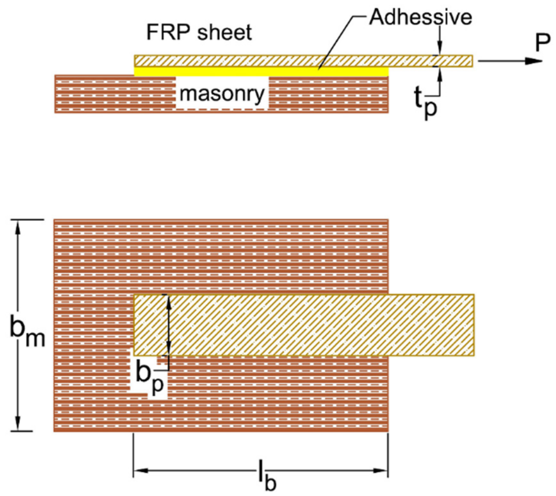

Figure 1. Adhesive-bonded joint [24].

In the area of empirical modeling, soft computing methods can be assumed as the effective superseded to usual techniques. Genetic programming (GP) [26] is a rather new soft computing method for the treatment modeling of structural engineering problems. GP is a development of genetic algorithms (GA). The major benefit of the GP-based procedures is their capability to create estimation equations without presuming a prior form of the relation.

Genetic programming (GP), and its deployment of gene expression programming (GEP), may be applied as an alternative to a physical model. In the last decade, new procedures based on GEP have been applied to civil engineering problems. Abdellahi et al. [27] proposed a new formula for bond strength of FRP-to-concrete composite joints using GEP. Kara [28] introduced a simple model to compute the concrete shear strength of FRP-reinforced concrete slender beams without stirrups using GEP. Chen et al. [29] used GEP to predict the slump flow of high-performance concrete by using seven concrete components. Cevik [30] used several soft computing approaches for predicting strength enhancement of FRP confined concrete cylinders. Additionally, Mansouri et al. [31] employed several soft computing approaches for the prediction of the peak and residual conditions of actively-confined concrete. However, each model agrees well with the experimental results from which it is gathered, but the model does not indicate good agreement with the other experimental results. Hence, it is necessary to develop analytical equations that can predict the debonding strength for masonry members retrofitted with FRP with a wide range of experimental data. Güneyisi et al. [32] suggested a new equation for the flexural overstrength factor for steel beams. Gandomi et al. [33] proposed a novel formulation for the strength of concrete under triaxial compression loading using GEP. The application of GEP tools can also be seen in other branches of civil engineering: Aytek and Kisi [34] used a GP approach for modeling suspended sediment. Azamathulla and Ghani [35] used GP to predict river pipeline scour. Shiri and Kisi [36] predicted short-term fluctuations of groundwater table depth by using GP. Azamathulla et al. [37] used GP approaches for modelling bridge pier scour. Shiri et al. [38] applied GEP for estimating daily reference evapotranspiration. Gandomi et al. [39] predicted the flow number of dense asphalt-aggregate mixtures using GEP. To the knowledge of the authors, the applicability of the GEP approach for predicting the debonding force of FRP-retrofitted masonry elements has not been investigated and/or published in the literature.

The main aim of this paper is to investigate the capability of GEP to predict the debonding resistance of FRP-retrofitted masonry structures. The accuracy of the GEP model is compared with experimental data and other existing models.

2. Shear Strength Contribution of FRP

The shear strength of FRPs is dependent on several factors, e.g., width of the FRP strip (b_p), thickness of the FRP strip (t_p), tensile strength of the masonry block (f_{ut}), Young's modulus of the FRP (E_p), width of the masonry block (b_m), and bonded length (l_b).

Table 1 shows several bond strength models which can be utilized for masonry. To improve the models for utilizing with masonry, the compressive strength (f'_{cm}) is represented as a function of the tensile strength (f_{ut}) of masonry in *MPa* units as:

$$f_{ut} = 0.53\sqrt{f'_{cm}} \quad (1)$$

Table 1. Analytical models for the evaluation of the (fiber-reinforced polymer) FRP-masonry bond strength.

Model	Equation (Units: N, mm)	References
Tanaka	$P_{\max} = l_b\, b_p(6.13 - \ln l_b)$	[40]
Sato	$P_{\max} = 2.68 \times 10^{-5}\,(f'_{cm})^{0.2}\, E_p\, t_p l_e (b_p + 7.4)$ $l_e = 1.89\,(E_p\, t_p)^{0.4} \quad if\ l_b > l_e : l_e = l_b$	[41]
Iso	$P_{\max} = 0.93\,(f'_{cm})^{0.44}\, l_e\, b_p$ $l_e = 0.125\,(E_p\, t_p)^{0.57} \quad if\ l_b > l_e : l_e = l_b$	[41]
Yang	$P_{\max} = \left(0.5 + 0.08\sqrt{0.01 E_p\, t_p/f_{ut}}\right) L_e\, b_p f_{ut}/2$ $l_e = 100\,\text{mm}$	[41]
Neubauer	$P_{\max} = \begin{cases} 0.64 k_p\, b_p \sqrt{E_p t_p f_{ut}} & l_b \geq l_e \\ 0.64 k_p\, b_p \sqrt{E_p t_p f_{ut}}\,\alpha & l_b < l_e \end{cases}$ $\alpha = \left(\frac{l_b}{l_e}\right)\left(2 - \frac{l_b}{l_e}\right) \quad l_e = \sqrt{\frac{E_p t_p}{2 f_{ut}}}$ $k_p = \sqrt{1.125\frac{2 - b_p/b_m}{1 + b_p/400}}$	[42]
Willis	$P_{\max} = 1.45\varphi_f^{0.263} f_{ut}^{0.6}\sqrt{l_{per} E_p t_p l_b}$ $\varphi_f = 1/(2 + b_p)$ for EB case $L_{per} = 2 + b_p$	[43]
Kashyap	$P_{\max} = 13.69\varphi_f^{0.84} f_{ut}^{0.9}\sqrt{l_{per} E_p t_p l_b}$ $\varphi_f = 1/(2 + b_p)$ for EB case $L_{per} = 2 + b_p$	[44]
Maeda	$P_{\max} = 110.2 \times 10^{-6}\, E_p\, t_p l_e\, b_p$ $l_e = e^{6.134 - 0.58 \times \ln(E_p\, t_p)}$ (unit of E_p is GPa)	[40]

Table 1. *Cont.*

Model	Equation (Units: N, mm)	References
Khalifa	$P_{\max} = 110.2 \times 10^{-6} \times (f'_{cm}/42)^{2/3} E_p t_p l_e b_p$ $l_e = e^{6.134 - 0.58 \times \ln(E_p t_p)}$ (unit of E_p is GPa)	[45]
De Lorenzis	$P_{\max} = b_p \sqrt{2E_p t_p G_c}$ $G_c = 1.43\,\mathrm{Nmm/mm^2}$	[46]
Van Gemert	$P_{\max} = 0.5 l_b b_p f_{ut}$	[42]
Dai	$P_{\max} = (b_p + 7.4)\sqrt{2E_p t_p G_c}$ $G_c = 0.514 f'^{0.236}_{cm}$	[47]
Accardi	$P_{\max} = b_p \sqrt{12 E_p t_p \sqrt{f'_{cm}}}$	[22]

3. Overview of Genetic Programming

Genetic programming is an expansion of John Holland's genetic algorithm [48], in which the population consists of computer programs of different sizes and shapes [26]. It supplies a solution in the form of a tree structure or in the form of a compressed equation using the certain dataset. More details may be found in Koza [26]. Gene expression programming (GEP), which is an expansion of GP [26], is a search method that requires computer programs (e.g., mathematical expressions, decision trees, polynomial constructs, and logical expressions). GEP computer programs are all encoded in linear chromosomes, which are then represented or translated into expression trees [49].

The advantages of GEP can be emphasized as follows: the chromosomes are simple entities: linear, compact, comparatively small, and easy to manage genetically. The expression trees are, individually, the expression of their respective chromosomes; they are the existence upon which choice acts and, according to fitness, they are selected to repeat, with correction. During reproduction it is the chromosomes of the individuals, not the expression trees, which are reproduced with correction and transmitted to the next generation [50]. More details about GEP can be found in [26].

4. Results and Discussion

The performance of GEP in training and testing sets is evaluated in terms of two usual statistical measures: correlation coefficient (R) and root mean square error (RMSE), which are given as follows:

$$\mathrm{RMSE} = \sqrt{\frac{1}{N}\sum_{i=1}^{N}(t_i - o_i)^2} \tag{2}$$

$$R = \sqrt{1 - \frac{\sum_{i=1}^{N}(t_i - o_i)^2}{\sum_{i=1}^{N}(o_i - \bar{o}_i)^2}} \tag{3}$$

in which t_i denotes the target values of the maximum debonding force; while o_i and $\bar{o}_i$ denote the observed and averaged observed values of the maximum debonding force, respectively; and N is the number of samples.

A new formulation of debonding strength for masonry elements retrofitted with FRP was derived using an experimental database from Kashyap et al. [44]. Table 2 lists 134 data points that were considered in this study. In the GEP model, b_p, t_p, E_p, f_{ut}, b_m, and l_b were considered as inputs and the maximum debonding force ($P_{\max}$) as the independent output. Data were randomly grouped into two subsets: a training set of 100 data points and a testing set of 34 data points—approximately 75% and 25% of the 134 data points, respectively.

Table 2. Database for FRP-reinforced masonry members (from Kashyap et al. [44]).

References	No.	t_p (mm)	E_p (GPa)	b_p (mm)	l_b (mm)	b_m (mm)	f_{ut} (MPa)	$P_{\max}$ (kN)
[51]	1	6.35	40.8	6.35	254	230	1.93	19.17
	2	6.35	40.8	6.35	381	230	1.93	18.55
[52]	3	1	22.3	25	50	400	2.05	4.88
	4	1	22.3	25	50	400	2.05	5.63
	5	1	22.3	25	50	400	2.05	4.25
	6	1	22.3	25	50	400	2.05	3.75
	7	1	22.3	25	50	400	2.05	5.13
	8	1	22.3	25	75	400	2.05	5.81
	9	1	22.3	25	75	400	2.05	5.44
	10	1	22.3	25	75	400	2.05	6.38
	11	1	22.3	25	75	400	2.05	3.94
	12	1	22.3	25	75	400	2.05	7.13
	13	1	22.3	25	100	400	2.05	4.75
	14	1	22.3	25	100	400	2.05	5
	15	1	22.3	25	100	400	2.05	6.5
	16	1	22.3	25	100	400	2.05	7.25
	17	1	22.3	25	100	400	2.05	7.25
	18	1	22.3	25	100	400	2.05	8.5
	19	1	22.3	25	50	200	2.73	9.25
	20	1	22.3	25	50	200	2.73	7.38
	21	1	22.3	25	50	200	2.73	8.63
	22	1	22.3	25	50	200	2.73	6.88
	23	1	22.3	25	75	200	2.73	10.69
	24	1	22.3	25	75	200	2.73	8.44
	25	1	22.3	25	75	200	2.73	9.38
	26	1	22.3	25	75	200	2.73	9.56
	27	1	22.3	25	75	200	2.73	8.25
	28	1	22.3	25	100	200	2.73	8.5
	29	1	22.3	25	100	200	2.73	10
	30	1	22.3	25	100	200	2.73	10
	31	1	22.3	25	100	200	2.73	9
	32	1	22.3	25	100	200	2.73	10
	33	1	22.3	25	100	400	2.05	5.58
	34	1	22.3	25	100	200	2.73	9.4
[53]	35	1	61	25	125	280	1.3	4.06
	36	1	61	50	100	280	1.3	5.9
	37	1	61	50	125	280	1.3	5.14
[54]	38	1.2	165	50	210	230	2.75	25.25
	39	1.2	165	50	280	230	2.75	28.4
[55]	40	2.8	207	15	355	230	3.57	61.6
	41	2.8	207	15	355	230	3.57	65.24
	42	2.8	207	15	355	230	3.57	63.53
	43	2.8	207	15	355	230	3.57	66.52
[56]	44	0.17	230	50	200	250	3.35	15.94
	45	0.17	230	50	200	250	3.35	17.12
	46	0.17	230	50	200	250	3.35	17.66
	47	0.17	230	50	200	250	3.35	19.61
	48	0.17	230	50	200	250	3.35	20.15
	49	0.23	65	50	200	250	3.35	11.69
	50	0.23	65	50	200	250	3.35	13.97
	51	0.23	65	50	200	250	3.35	13.65
	52	0.23	65	50	200	250	3.35	13.2
	53	0.23	65	50	200	250	3.35	14.18
[57]	54	2.8	207	15	336	230	3.57	83.45
	55	2.8	207	15	336	230	3.57	71.09
	56	2.8	207	15	336	230	3.57	81.48
	57	2.8	207	15	336	230	3.57	70.36
	58	2.8	207	15	336	230	3.57	59.41
	59	2.8	207	15	336	230	3.57	63.88
	60	2.8	207	15	336	230	3.57	69.41
	61	2.8	207	15	336	230	3.57	84.5

Table 2. *Cont.*

References	No.	t_p (mm)	E_p (GPa)	b_p (mm)	l_b (mm)	b_m (mm)	f_{ut} (MPa)	$P_{\max}$ (kN)
[43]	62	1.2	162	15	241	230	3.55	46.8
	63	1.2	162	15	328	230	3.55	44
	64	1.2	162	15	328	230	3.55	38.3
	65	1.2	162	15	334	230	3.55	46.7
	66	1.2	162	20	328	230	3.55	50
	67	1.2	162	20	328	230	3.55	51.2
	68	2	65	50	420	230	3.55	22.1
	69	2	65	50	395	230	3.55	21.5
	70	2	65	50	419	230	3.55	21.9
	71	2	65	50	396	230	3.55	18.1
	72	2	65	50	394	230	3.55	24.7
	73	2	65	50	393	230	3.55	24.3
	74	0.62	73	50	386	230	3.55	19.9
	75	0.62	73	50	386	230	3.55	18.6
	76	1.2	162	50	140	230	3.55	26.8
	77	1.2	162	50	210	230	3.55	24.9
	78	1.2	162	50	280	230	3.55	28.4
	79	0.15	80.2	25	150	235	1.57	3.48
	80	0.15	80.2	25	150	235	1.57	4.81
[58]	81	0.15	80.2	25	150	235	1.57	4.69
	82	0.15	80.2	25	150	235	1.57	4.64
	83	0.15	80.2	25	100	235	1.57	3.66
	84	0.15	80.2	25	100	235	1.57	3.17
	85	0.15	80.2	25	100	235	1.57	2.85
	86	0.15	80.2	25	100	235	1.57	3.68
	87	0.15	80.2	25	100	235	1.57	3.79
	88	0.15	80.2	25	200	235	1.57	4.48
	89	0.15	80.2	25	200	235	1.57	5.06
	90	0.15	80.2	25	150	235	1.57	5.27
	91	0.15	80.2	25	150	235	1.57	4.2
	92	0.15	80.2	25	150	235	1.57	4.89
	93	0.15	80.2	25	150	235	1.57	5.6
	94	0.15	80.2	25	150	235	1.57	4.34
	95	0.15	80.2	25	150	235	1.57	5.49
	96	0.15	80.2	25	150	235	1.57	3.52
	97	0.15	80.2	25	150	235	1.57	4.83
	98	0.15	80.2	25	150	235	1.57	4.53
	99	0.15	80.2	25	150	235	1.57	5.46
	100	0.15	80.2	25	150	235	1.57	4.55
	101	0.15	80.2	25	150	235	1.57	3.73
	102	0.15	80.2	25	150	235	1.57	3.82
	103	0.15	80.2	25	150	235	1.57	4.54
	104	0.15	80.2	25	150	235	1.57	4.06
	105	0.12	216	25	150	235	1.57	4.78
	106	0.12	216	25	150	235	1.57	4.29
	107	0.12	216	25	150	235	1.57	4.02
	108	0.12	216	25	150	235	1.57	4.33
	109	0.12	216	25	150	235	1.57	4.26
[59]	110	0.13	230	50	150	740	1.0236	5.04
	111	0.13	230	50	150	740	0.80901	3.92
	112	0.13	230	50	150	740	0.780739	4.66
	113	0.13	230	50	150	740	0.897877	4.28
	114	0.13	230	50	150	740	1.077087	4.73
	115	0.13	230	50	150	740	1.107941	4.83
	116	0.13	230	50	150	740	0.991539	3.89
	117	0.13	230	50	150	740	0.99578	4.01
	118	0.13	230	50	150	740	0.905664	4.2
	119	0.13	230	50	100	740	1.091337	4.93
	120	0.13	230	50	100	740	0.901	4.25
	121	0.13	230	50	100	740	0.981574	4.43
	122	0.13	230	50	100	740	1.03723	4.61

Table 2. *Cont.*

References	No.	t_p (mm)	E_p (GPa)	b_p (mm)	l_b (mm)	b_m (mm)	f_{ut} (MPa)	$P_{\max}$ (kN)
	123	0.13	230	50	100	740	0.943638	4.07
	124	0.13	230	50	100	740	1.002807	3.28
	125	0.13	230	50	100	740	1.012564	4.65
	126	0.13	230	50	100	740	0.96425	3.35
	127	0.13	230	50	50	740	0.921042	2.28
	128	0.13	230	50	50	740	1.048007	2.31
	129	0.13	230	50	50	740	1.353317	4.73
	130	0.13	230	50	50	740	0.914922	2.22
	131	0.13	230	50	50	740	0.954	2.33
	132	0.13	230	50	50	740	0.970059	2.2
	133	0.13	230	50	50	740	1.079692	2.13
	134	0.13	230	50	50	740	0.890021	3.51

The statistical analyses of the data are summarized in Table 3. As can be observed in Table 3, the statistics for both the training and testing sets are in good agreement, meaning that both of them represent almost similar populations.

Table 4 shows the functional set and operational parameters used in GEP modeling.

The GEP-based explicit formulation of maximum load is given in the following equation:

$$P_{\max} = [f_{ut}^{1.5} L_b - L_b t_p c_1] + [f_{ut}^3 b_m - b_p^2 t_p] + [L_b^{1.5} + c_2 + \frac{t_p}{c_0}(L_b + E_p)] \tag{4}$$

in which c_1 = 9.941346, c_2 = 9.58728, and c_0 = 9.351684.

The variation of observed and estimated values by GEP model are illustrated in Figure 2 for the training and test periods. It is clear from the figure that the GEP estimates closely follow the corresponding observed experimental data in the both periods. The scatterplots of the observed and estimated debonding forces are shown in Figure 3. From the fit line and R^2 values, it is evident that the estimates of the GEP model are very close to the ideal line.

Table 5 shows the values of two performance indicators (R^2 and RMSE) for some existing models and the proposed model in this study, regarding both training and testing phases. According to a logical hypothesis [60], if a model gives $R > 0.8$, and the error value (e.g., RMSE) is at the minimum, there is a strong correlation between the computed and observed values. The model can, hence, be judged very well. As shown in Table 4, the proposed model predicted the debonding strength for both training and testing set with lower errors of RMSE (4013.1 and 3801.7), and higher accuracy (R^2 = 0.9647 and 0.9492), respectively. The RMSE values of the GEP and existing models are compared in Figures 4 and 5 for the training and test data. It is clear from the figures that the training and test results are parallel to the each other and the GEP model has the lowest RMSE in both training and test periods. Among the existing methods, Kashyap performs better than the other models.

It can be observed from Table 5 and Figure 3 that the GEP model with high R and low RMSE values accurately predicts the observed values. Meanwhile, it is significant that the error values are not only low but also as similar as feasible for the training and testing sets, which infers that the suggested model has both predictive ability and generalization efficiency [60].

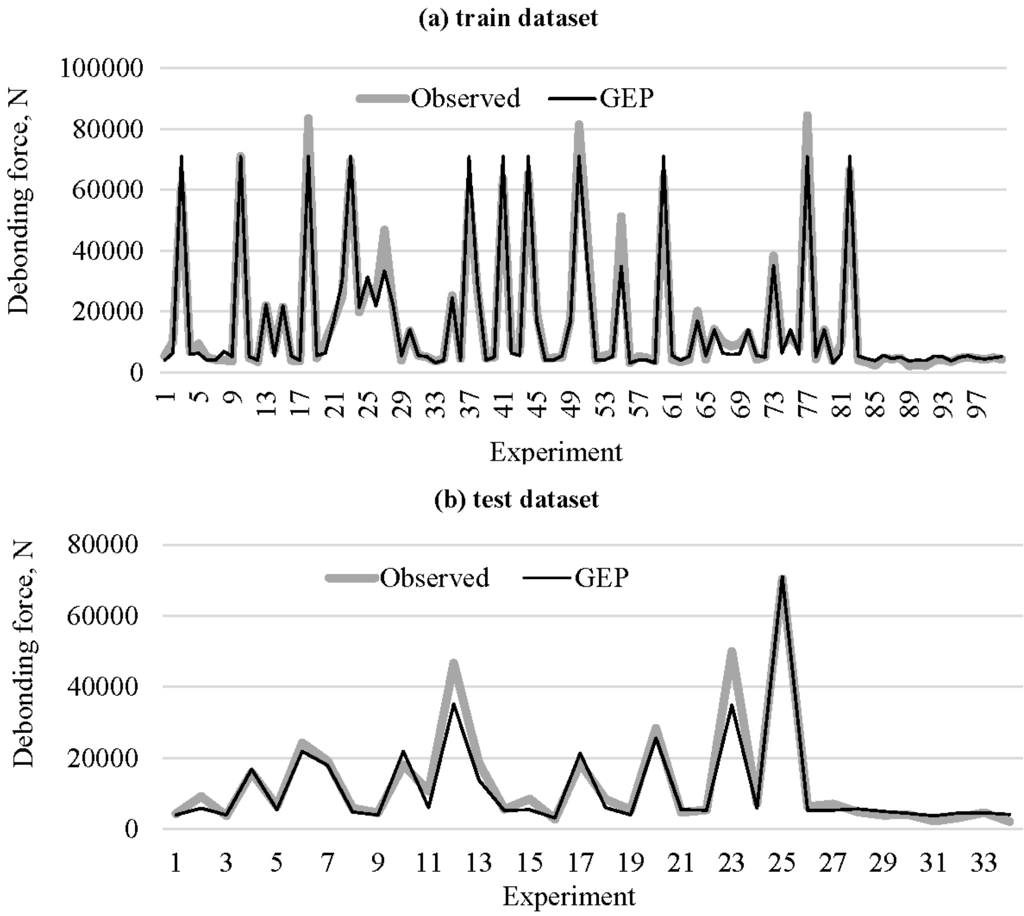

Figure 2. Observed and predicted debonding forces by GEP (gene expression programming) for (**a**) training dataset and (**b**) testing dataset.

Table 3. Statistics for the experimental data.

	b_m (mm)	b_p (mm)	E_p (GPa)	f_{ut} (MPa)	l_b (mm)	t_p (mm)	$P_{\max}$ (kN)
Training data							
Mean	224.90	23.98	126.49	2.11	162.76	133.98	16.52
Standard deviation	79.72	15.43	82.62	1.22	108.89	285.37	21.37
Min. value	50.00	0.78	22.30	0.13	50.00	0.12	2.20
Max. value	400.00	50.00	230.00	3.57	420.00	740.00	84.50
Testing data							
Mean	237.50	22.63	103.76	1.96	154.79	153.43	13.01
Standard deviation	100.80	16.07	84.95	1.17	122.95	303.16	15.33
Min. value	50.00	0.81	22.30	0.13	50.00	0.15	2.13
Max. value	400.00	50.00	230.00	3.57	396.00	740.00	70.36

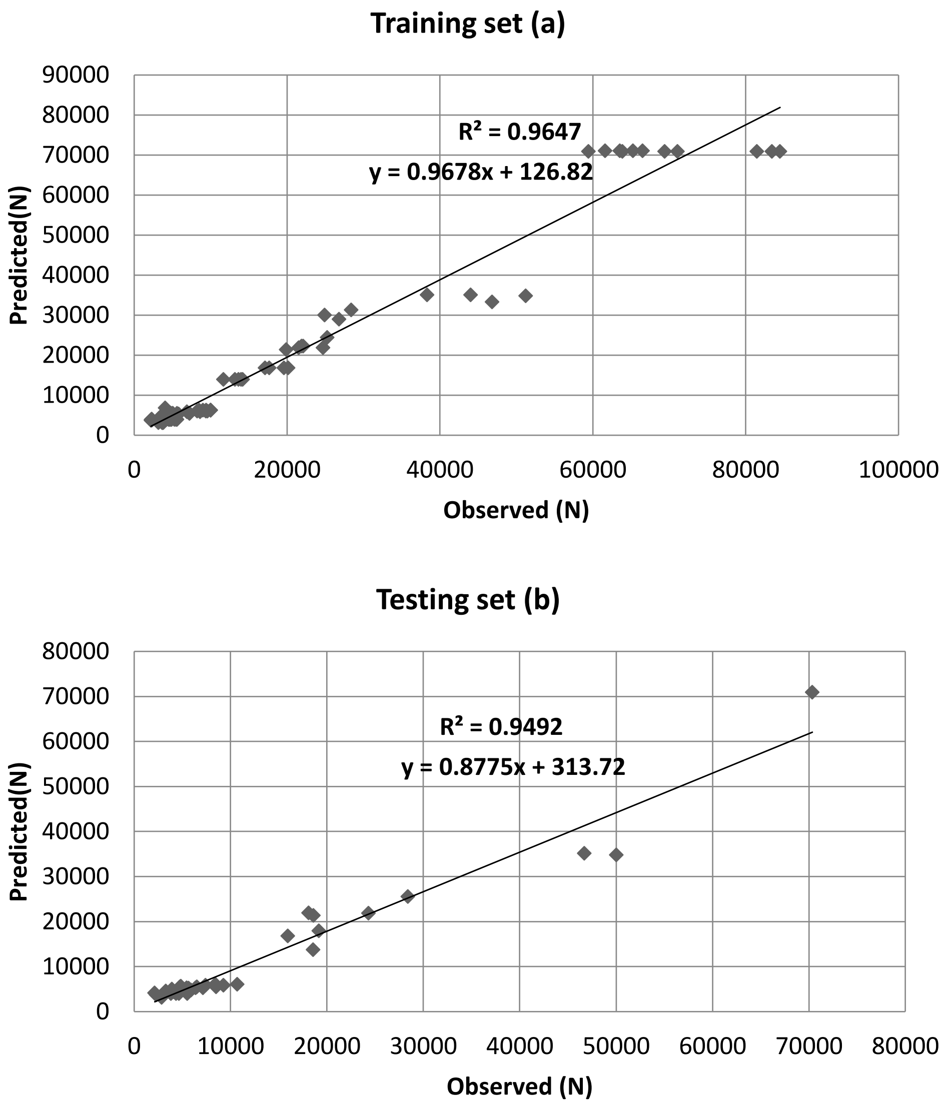

Figure 3. Observed and predicted debonding forces by GEP for (**a**) training and (**b**) testing data.

Table 4. General parameters of the applied GEP (gene expression programming) models.

Number of chromosomes	30	One point recombination rate	0.3
Head size	8	Two point recombination rate	0.3
Number of genes	3	Gene recombination rate	0.1
Linking function	addition	Gene transposition rate	0.1
Fitness function error type	RRSE	Insertion sequence transposition rate	0.1
Mutation rate	0.044	Root insertion sequence transposition	0.1
Inversion rate	0.1	-	-

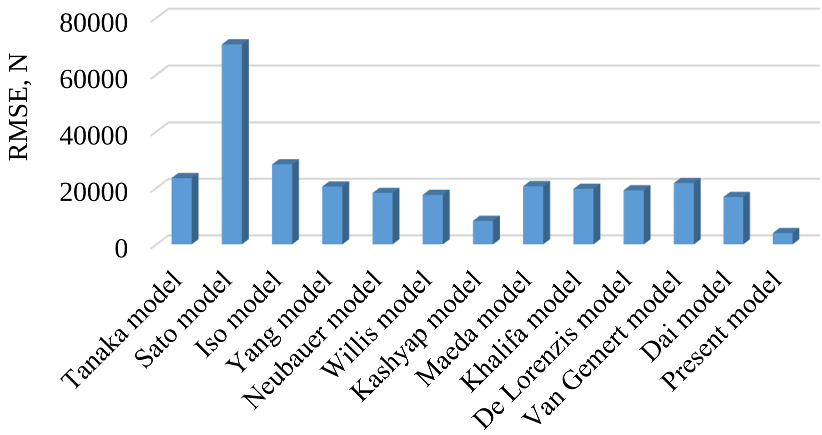

Figure 4. Comparison of the GEP model with existing methods in the prediction of the debonding force for the training data.

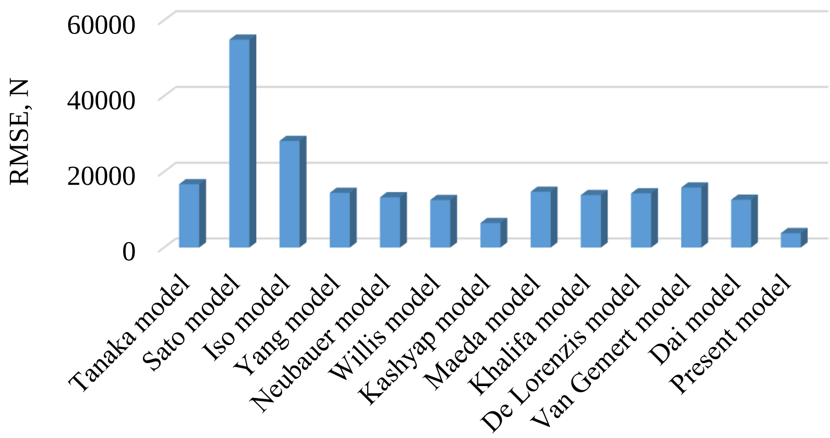

Figure 5. Comparison of GEP model with existing methods in the prediction of the debonding force for the testing data.

Table 5. Training and testing results of existing models and GEP.

Model	Training Data		Test Data	
	R^2	RMSE (root mean square errors)	R^2	RMSE
Tanaka model	0.1722	23,485.3	0.1088	16,711.0
Sato model	0.8445	70,656.6	0.6723	54,877.9
Iso model	0.0783	28,333.3	0.1179	28,139.8
Yang model	0.4974	20,474.6	0.2124	14,444.9
Neubauer model	0.4014	18,200.2	0.3190	13,263.4
Willis model	0.6045	17,555.1	0.4898	12,535.5
Kashyap model	0.9189	8309.8	0.8841	6471.9
Maeda model	0.2132	20,622.8	0.1624	14,723.3
Khalifa model	0.3209	19,669.1	0.2833	13,847.4
De Lorenzis model	0.2988	19,160.5	0.2168	14,304.8
Van Gemert model	0.0827	21,723.1	0.1204	15,851.3
Dai model	0.5013	16,790.5	0.3837	12,609.5
Present model	0.9647	4013.1	0.9492	3801.7

5. Conclusions

In this study, GEP was applied to model the complex behavior of debonding strength of FRP strengthened masonry (SM) elements. The major focus of this research is to propose a novel formula for determining the debonding resistance of FRP SM members as a function of various influencing factors. A reliable database including formerly published debonding strength of FRP SM members test results was used for developing the applied model. The suggested model used various important parameters (b_p, t_p, E_p, f_{ut}, b_m, l_b) representing the behavior of the debonding strength as inputs. The GEP results revealed good agreement with the gathered experimental results. The performance of the GEP was compared to the twelve existing empirical models obtained in previous studies. GEP was found to be the best model in prediction of the debonding strength of retrofitted masonry members. Among the empirical models, Kashyap provided the best results. The optimal GEP model reduced the root mean square errors by 51.7% and 41.3% with respect to the best empirical model (Kashyap) in the training and test periods, respectively. The proposed GEP model can be applied in practical pre-planning and design purposes because it was obtained from experimental tests on beams with a wide range of geometrical and mechanical properties.

Acknowledgments: This research was supported by a grant (15TBIP-C093001-01) from Support for Infrastructure and transportation technology commercialization Program funded by Ministry of Land, Infrastructure and Transport of Korean government. The authors gratefully acknowledge this support.

Author Contributions: For research articles with several authors, a short paragraph specifying their individual contributions must be provided. The following statements should be used. Iman Mansouri and Ozgur Kisi collected many experimental specimens and applied artificial tools to database and Prof. Jong Wan Hu analyzed the data; Jong Wan Hu contributed reagents/materials/analysis tools; Iman Mansouri wrote the paper.

Conflicts of Interest: The authors declare no conflict of interest.

References

1. Maruccio, C. Numerical Analysis of FRP Strengthened Masonry Structures. Ph.D. Thesis, University of Minho, Portugal and Sapienza University of Rome, Rome, Italy, 2010.
2. Brencich, A.; Gambarotta, L. Mechanical response of solid clay brickwork under eccentric loading. Part ii: Cfrp reinforced masonry. *Mater. Struct.* **2005**, *38*, 267–273. [CrossRef]
3. Grande, E.; Milani, G.; Sacco, E. Modelling and analysis of FRP-strengthened masonry panels. *Eng. Struct.* **2008**, *30*, 1842–1860. [CrossRef]
4. Grande, E.; Imbimbo, M.; Sacco, E. Bond behaviour of CFRP laminates glued on clay bricks: Experimental and numerical study. *Compos. Part B: Eng.* **2011**, *42*, 330–340. [CrossRef]
5. Marfia, S.; Sacco, E. Modeling of reinforced masonry elements. *Int. J. Solids Struct.* **2001**, *38*, 4177–4198. [CrossRef]
6. Albert, M.; Elwi, A.; Cheng, J. Strengthening of unreinforced masonry walls using FRPs. *J. Compos. Constr.* **2001**, *5*, 76–84. [CrossRef]
7. Bajpai, K.; Kuthinh, D. Bending performance of masonry walls strengthened with near-surface mountedFRP bars. In Proceedings of the 9th North American Masonry Conference, Clemson, SC, USA, 1–4 June 2003.
8. Carney, P.; Myers, J.J. Shear and flexural strengthening of masonry infill walls with FRP for extreme out-of-plane loading. In *Architectural Engineering*; ASCE: Austin, TX, USA, 2003.
9. Galati, N.; Tumialan, G.; Nanni, A. Strengthening with FRP bars of urm walls subject to out-of-plane loads. *Constr. Build. Mater.* **2006**, *20*, 101–110. [CrossRef]
10. Hamoush, S.A.; McGinley, M.W.; Mlakar, P.; Scott, D.; Murray, K. Out-of-plane strengthening of masonry walls with reinforced composites. *J. Compos. Constr.* **2001**, *5*, 139–145. [CrossRef]
11. Kuzik, M.; Elwi, A.; Cheng, J. Cyclic flexure tests of masonry walls reinforced with glass fiber reinforced polymer sheets. *J. Compos. Constr.* **2003**, *7*, 20–30. [CrossRef]
12. Lunn, D.S. Behavior and Modeling of Infill Masonry Walls Strengthened with FRP Using Various end Anchorage. Ph.D. Thesis, North Carolina State University, Raleigh, NC, USA, 2013.
13. Patoary, M.K.H.; Tan, K.H. Blast resistance of prototype in-build masonry walls strengthened with FRP systems. In Proceedings of the 6th International Symposium on FRP Reinforcement for Concrete Structures, Singapore, Singapore, 8–10 July 2003.
14. Roca, P.; Araiza, G. Shear response of brick masonry small assemblages strengthened with bonded FRP laminates for in-plane reinforcement. *Constr. Build. Mater.* **2010**, *24*, 1372–1384. [CrossRef]

15. Velazquez-Dimas, J.I.; Ehsani, M.R. Modeling out-of-plane behavior of urm walls retrofitted with fiber composites. *J. Compos. Constr.* **2000**, *4*, 172–181. [CrossRef]
16. Fam, A.Z.; Rizkalla, S.H.; Tadros, G. Behavior of CFRP for prestressing and shear reinforcements of concrete highway bridges. *ACI Struct. J.* **1997**, *94*, 77–86.
17. Kolsch, H. Carbon fiber cement matrix (cfcm) overlay system for masonry strengthening. *J. Compos. Constr.* **1998**, *2*, 105–109. [CrossRef]
18. Triantafillou, T.C. Strengthening of masonry structures using epoxy-bonded FRP laminates. *J. Compos. Constr.* **1998**, *2*, 96–104. [CrossRef]
19. Al-Salloum, Y.A.; Almusallam, T.H. Load capacity of concrete masonry block walls strengthened with epoxy-bonded gfrp sheets. *J. Compos. Mater.* **2005**, *39*, 1719–1745. [CrossRef]
20. Wang, Q.; Chai, Z.; Huang, Y.; Huang, Y.; Yang, Y.; Zhang, Y. Seismic shear capacity of brick masonry wall reinforced by GFRP. *Asian J. Civil Eng.* **2006**, *7*, 563–580.
21. Stratford, T.; Pascale, G.; Manfroni, O.; Bonfiglioli, B. Shear strengthening masonry panels with sheet glass-fiber reinforced polymer. *J. Compos. Constr.* **2004**, *8*, 434–443. [CrossRef]
22. Accardi, M.; Cucchiara, C.; La Mendola, L. Bond behavior between cfrp strips and calcarenite stone. In Proceedings of the 6th International Conference on Fracture Mechanics of Concrete and Concrete Structures, Catania, Italy, 17–22 June 2007; pp. 1203–1211.
23. Milani, G.; Rotunno, T.; Sacco, E.; Tralli, A. Failure load of FRP strengthened masonry walls: Experimental results and numerical models. *Struct. Durab. Health Monit.* **2006**, *2*, 29–50.
24. Mansouri, I.; Kisi, O. Prediction of debonding strength for masonry elements retrofitted with FRP composites using neuro fuzzy and neural network approaches. *Compos. Part B: Eng.* **2015**, *70*, 247–255. [CrossRef]
25. Sharma, B. Debonding Failure of Fiber Reinforced Polymers. Master's Thesis, University of Hawaii at Manoa, Honolulu, HI, USA, 2006.
26. Koza, J.R. *Genetic Programming: On the Programming of Computers by Means of Natural Selection*; MIT Press: Cambridge, MA, USA, 1992.
27. Abdellahi, M.; Heidari, J.; Bahmanpour, M. A new predictive model for the bond strength of FRP-to-concrete composite joints. *Struct. Concr.* **2014**, *15*, 509–521. [CrossRef]
28. Kara, I.F. Prediction of shear strength of FRP-reinforced concrete beams without stirrups based on genetic programming. *Adv. Eng. Softw.* **2011**, *42*, 295–304. [CrossRef]
29. Chen, L.; Kou, C.-H.; Ma, S.-W. Prediction of slump flow of high-performance concrete via parallel hyper-cubic gene-expression programming. *Eng. Appl. Artif. Intell.* **2014**, *34*, 66–74. [CrossRef]
30. Cevik, A. Modeling strength enhancement of FRP confined concrete cylinders using soft computing. *Expert Syst. Appl.* **2011**, *38*, 5662–5673. [CrossRef]
31. Mansouri, I.; Gholampour, A.; Kisi, O.; Ozbakkaloglu, T. Evaluation of peak and residual conditions of actively confined concrete using neuro-fuzzy and neural computing techniques. *Neural Comput. Appl.* **2016**, 1–16. [CrossRef]
32. Güneyisi, E.M.; D'Aniello, M.; Landolfo, R.; Mermerdaş, K. A novel formulation of the flexural overstrength factor for steel beams. *J. Construct. Steel Res.* **2013**, *90*, 60–71. [CrossRef]
33. Gandomi, A.H.; Babanajad, S.K.; Alavi, A.H.; Farnam, Y. Novel approach to strength modeling of concrete under triaxial compression. *J. Mater. Civil Eng.* **2012**, *24*, 1132–1143. [CrossRef]
34. Aytek, A.; Kişi, Ö. A genetic programming approach to suspended sediment modelling. *J. Hydrol.* **2008**, *351*, 288–298. [CrossRef]
35. Azamathulla, H.M.; Ghani, A.A. Genetic programming to predict river pipeline scour. *J. Pipeline Syst. Eng. Pract.* **2010**, *1*, 127–132. [CrossRef]
36. Shiri, J.; Kişi, Ö. Comparison of genetic programming with neuro-fuzzy systems for predicting short-term water table depth fluctuations. *Comput. Geosci.* **2011**, *37*, 1692–1701. [CrossRef]
37. Azamathulla, H.M.; Ghani, A.A.; Zakaria, N.A.; Guven, A. Genetic programming to predict bridge pier scour. *J. Hydraul. Eng.* **2010**, *136*, 165–169. [CrossRef]
38. Shiri, J.; Kişi, Ö.; Landeras, G.; López, J.J.; Nazemi, A.H.; Stuyt, L.C.P.M. Daily reference evapotranspiration modeling by using genetic programming approach in the basque country (northern spain). *J. Hydrol.* **2012**, *414–415*, 302–316. [CrossRef]
39. Gandomi, A.H.; Alavi, A.H.; Mirzahosseini, M.R.; Nejad, F.M. Nonlinear genetic-based models for prediction of flow number of asphalt mixtures. *J. Mater. Civil Eng.* **2011**, *23*, 248–263. [CrossRef]

40. Chen, J.F.; Teng, J.G. Anchorage strength models for FRP and steel plates bonded to concrete. *J. Struct. Eng.* **2001**, *127*, 784–791. [CrossRef]
41. Sayed-Ahmed, E.Y.; Bakay, R.; Shrive, N.G. Bond strength of FRP laminates to concrete: State-of-the-art review. *Electron. J. Struct. Eng.* **2009**, *9*, 45–61.
42. D'Antino, T.; Pellegrino, C. Bond between FRP composites and concrete: Assessment of design procedures and analytical models. *Compos. Part B: Eng.* **2014**, *60*, 440–456. [CrossRef]
43. Willis, C.R.; Yang, Q.; Seracino, R.; Griffith, M.C. Bond behaviour of FRP-to-clay brick masonry joints. *Eng. Struct.* **2009**, *31*, 2580–2587. [CrossRef]
44. Kashyap, J.; Willis, C.R.; Griffith, M.C.; Ingham, J.M.; Masia, M.J. Debonding resistance of FRP-to-clay brick masonry joints. *Eng. Struct.* **2012**, *41*, 186–198. [CrossRef]
45. Khalifa, A.; Gold, W.J.; Nanni, A.; M.I., A.A. Contribution of externally bonded FRP to shear capacity of rc flexural members. *J. Compos. Constr.* **1998**, *2*, 195–202. [CrossRef]
46. Laura De Lorenzis, B.M.; Antonio, N. Bond of fiber-reinforced polymer laminates to concrete. *Mater. J.* **2001**, *98*, 256–264.
47. Dai, J.; Ueda, T.; Sato, Y. Development of the nonlinear bond stress–slip model of fiber reinforced plastics sheet–concrete interfaces with a simple method. *J. Compos. Constr.* **2005**, *9*, 52–62. [CrossRef]
48. Holland, J.H. *Adaptation in Natural and Artificial Systems*; University of Michigan Press: Ann Arbor, MI, USA, 1975.
49. Azamathulla, H.M.; Ahmad, Z.; Ghani, A.Ab. Computation of discharge through side sluice gate using gene-expression programming. *Irrig. Drain.* **2013**, *62*, 115–119. [CrossRef]
50. Ferreira, C. Gene expression programming in problem solving. In *Soft Computing and Industry: Recent Applications*; Roy, R., Köppen, M., Ovaska, S., Furuhashi, T., Hoffmann, F., Eds.; Springer: London, UK, 2002; pp. 635–653.
51. Turco, V.N.; Galati, L.; De Lorenzis Modena, C.; Nanni, A. Bond between near surface mounted FRP rods and masonry in structural strengthening. 2003, pp. 209–217. Available online: http://rb2c.mst.edu/media/research/rb2c/documents/BNSM.pdf (accessed on 2 November 2016).
52. Liu, Y.; Dawe, J.; McInerney, J. Behaviour of gfrp sheets bonded to masonry walls. In Proceedings of the International Symposium on Bond Behaviour of FRP in Structures, BBFS 2005, Hong kong, China, 2005; pp. 473–480.
53. Camli, U.S.; Binici, B. Strength of carbon fiber reinforced polymers bonded to concrete and masonry. *Constr. Build. Mater.* **2007**, *21*, 1431–1446. [CrossRef]
54. Xia, S.; Oehlers, D. Debonding mechanisms in FRP plated unreinforced masonry under out-of-plane loading. *Adv. Struct. Eng.* **2006**, *9*, 619–637. [CrossRef]
55. Konthesingha, K.M.C.; Masia, M.J.; Petersen, R.B.; Page, A.W. Bond behaviour of nsm FRP strips to modern clay brick masonry prisms under cyclic loading. In Proceedings of the 11th Canadian Masonry Symposium, Toronto, Canada, 31 May–3 June 2009.
56. Lam, C. Finite element study of bond-slip behaviour of cfrp and gfrp laminates on brick masonry. Master's Thesis, Universitat Politècnica de Catalunya, Barcelona, Spain, 2009.
57. Petersen, R.B.; Masia, M.J.; Seracino, R. Bond behavior of near-surface mounted FRP strips bonded to modern clay brick masonry prisms: Influence of strip orientation and compression perpendicular to the strip. *J. Compos. Constr.* **2009**, *13*, 169–178. [CrossRef]
58. Oliveira, D.V.; Basilio, I.; Loureņo, P.B. Experimental bond behavior of FRP sheets glued on brick masonry. *J. Compos. Constr.* **2011**, *15*, 32–41. [CrossRef]
59. La Mendola, L.; Failla, A.; Cucchiara, C.; Accardi, M. Debonding phenomena in CFRP strengthened calcarenite masonry walls and vaults. *Adv. Struct. Eng.* **2009**, *12*, 745–760. [CrossRef]
60. Gandomi, A.H.; Alavi, A.H.; Kazemi, S.; Gandomi, M. Formulation of shear strength of slender rc beams using gene expression programming, part i: Without shear reinforcement. *Autom. Constr.* **2014**, *42*, 112–121. [CrossRef]